Reduced sea ice concentrations in the Arctic Ocean during the last interglacial period revealed by sediment cores off northern Greenland

Niels Nørgaard-Pedersen,[1] Naja Mikkelsen,[1] Susanne Juul Lassen,[1] Yngve Kristoffersen,[2] and Emma Sheldon[1]

Received 13 February 2006; revised 21 August 2006; accepted 20 September 2006; published 9 March 2007.

[1] We present a record encompassing marine isotope stages 7-1 from a hitherto unexplored and heavily ice-covered area of the Arctic Ocean, the Lomonosov Ridge off the northern Greenland-Canada continental margin, using nannofossil and benthic foraminifera stratigraphy. Planktic foraminifera assemblages are used as a key paleoceanographic proxy, and a surprisingly large variability is found for an interior Arctic Ocean site. Abundant small (63–125 μm) subpolar *Turborotalita quinqueloba* occur in two sections, possibly representing substages 5e (last interglacial) and 5a (warm interstadial). However, the present-day circulation pattern and the very distant location of high productive regions cannot explain such high abundances of subpolar specimens in the interior, perennially sea ice–covered Arctic Ocean. Hence our proxy record indicates that last interglacial sea ice concentrations were reduced off some areas of northern Greenland-Canada. Whether this was part of a larger regional pattern or it represents the influence of polynya areas with locally increased productivity remains to be solved. With respect to glacial conditions, increased ice-rafted debris (IRD) deposition in the area appears to be associated with glacial stages 6, 4, and late 3. Stage 2 sediments (including the Last Glacial Maximum) are condensed with a sparse IRD content only.

Citation: Nørgaard-Pedersen, N., N. Mikkelsen, S. J. Lassen, Y. Kristoffersen, and E. Sheldon (2007), Reduced sea ice concentrations in the Arctic Ocean during the last interglacial period revealed by sediment cores off northern Greenland, *Paleoceanography*, *22*, PA1218, doi:10.1029/2006PA001283.

1. Introduction

[2] The reduction and thinning of Arctic sea ice in recent decades [e.g., *ACIA Overview Report*, 2004; *Rothrock et al.*, 1999] has drawn attention to whether this environmental change is an early reaction to global warming, or if it is part of a natural multidecadal variation of the Arctic environment. Modeling studies of global warming effects indicate that the Arctic is likely to show a large temperature increase, and that sea ice cover, by the end of this century, could almost disappear during peak summer seasons [*Johannessen et al.*, 2004; Hadley Centre, http://www.metoffice.com/research/hadleycentre//models/modeldata.html, 2006]. Such a scenario would not only have a dramatic impact on the Arctic ecosystem, navigation, and indigenous people, but could also influence the thermohaline circulation and regional climate in the sub-Arctic and North Atlantic region. In this discussion, there is an urgent need for high-latitude Arctic records of climate, oceanography and sea ice cover representing long time periods and, in particular, records of natural environmental change during earlier warm periods.

[3] In spite of its importance, the recent geological record of the Arctic Ocean is still poorly known and hampered by difficult access, controversial chronostratigraphic models and limits in the applicability of traditionally used proxies. Time control for Arctic Ocean sequences beyond the range of ^{14}C-dating has mostly been based on crude magnetostratigraphy combined with lithostratigraphic correlation of characteristic sediment units. A distinct decrease in inclination occurring at a same stratigraphic level throughout the Arctic Ocean was, till recently, interpreted as the Brunhes-Matuyama boundary [e.g., *Clark et al.*, 1980; *Poore et al.*, 1993; *Spielhagen et al.*, 1997]. The succession of gray (mostly barren) and brown (fossiliferous) beds overlying this boundary has been interpreted as glacial-interglacial events, corresponding to marine oxygen isotope stages (MIS) 1 to 19 [*Poore et al.*, 1993; *Phillips and Grantz*, 1997; *Spielhagen et al.*, 1997]. However, by extending the established nannofossil stratigraphy from the northernmost Atlantic [*Gard*, 1988; *Gard and Backman*, 1990] to central Arctic records, *Jakobsson et al.* [2000, 2001] could show that the above decline in inclination is an excursion rather than inversion of magnetic field. This implies a much younger age of sediment, and accordingly, the possibility to detect stadial-interstadial variability of interior Arctic Ocean sediment records. Later, absolute dating of marine isotope stage 5 central Arctic Ocean sediments by optically stimulated luminescence (OSL) corroborated the new stratigraphic framework [*Jakobsson et al.*, 2003]. The central Arctic records can be further correlated to distant middepth Amerasian basin records by means of unique benthic

[1]Geological Survey of Denmark and Greenland, Copenhagen, Denmark.
[2]Department of Earth Science, University of Bergen, Bergen, Norway.

0883-8305/07/2006PA001283$12.00

foraminifera biostratigraphic events [*Polyak et al.*, 2004]. This stratigraphic framework implies that late Quaternary hemipelagic sedimentation rates for a number of interior Artic sites appear to have been in the order of a few cm/kyr rather than a few mm/kyr as earlier age models indicated [*Backman et al.*, 2004; *Spielhagen et al.*, 2004].

[4] This study documents a record from a hitherto unexplored, heavily ice-covered region of the Arctic Ocean: the southernmost part of the Lomonosov Ridge facing the Lincoln Sea north of Greenland and Ellesmere Island (Figure 1). By using a suite of different stratigraphic and paleoceanographic tools, we aim at the identification and interpretation of previous warm periods. Specifically, by studying planktic foraminifera assemblages >63 μm (including subpolar specimens) we are able to refine the paleoceanographic interpretation of interglacial events at an interior Arctic Ocean site. In order to enhance comparison with the late Holocene record (which is largely missing), we show faunal results from radiocarbon-dated surface sediment samples from the central Lomonosov Ridge and a site adjacent to the Morris Jesup Rise. Moreover, we attempt to identify events related to major glaciations of the adjacent northern Greenland and northern Canada continental margin, for which glaciation events beyond the Last Glacial Maximum is largely unknown.

2. Study Area

[5] Sediment coring and seismic reflection measurements were part of the multidisciplinary Greenland Arctic Shelf Ice and Climate Experiment (GreenICE) to study the structure and dynamics of the sea ice cover and attempt to relate these to a longer-term record of climate variability retrieved from the sediment cores. The field work was carried out during a two week campaign in May 2004 on drifting sea ice at 85° N, 65° W, ca. 170 km north of Ellesmere Island (Figure 1). Wind stresses from persistent easterly winds resulted in a drift trajectory of 245 ± 15° from a water depth of 550 m to about 1100 m over the southernmost part of the Lomonosov Ridge.

[6] The Lincoln Sea and the adjacent Arctic Ocean are generally considered to have some of the thickest sea ice cover of the entire Arctic Ocean, with mean ice thicknesses of 4 m or more [*Wadhams*, 1997; *Wadhams and Davis*, 2000]. Ice thickness measurements from helicopter flights around the GreenICE study area by a low-frequency electromagnetic induction (EMI) device confirmed mean sea ice thicknesses of 4–5 m during May 2004 [*Haas et al.*, 2006]. The present ice drift and surface water circulation over the study area (Figure 1) either recirculates in the Beaufort Gyre over the Canada Basin or bends off toward the east with the Transpolar Drift Current when approaching the north Greenland shelf, leading to ice convergence and heavy ice conditions.

[7] The stratified water mass structure of the Arctic Ocean includes the low-salinity surface water, several intermediate water layers, and the bottom waters [*Aagard et al.*, 1985]. The surface water receives a large river runoff that keeps the salinity low and thus, in addition to cold temperatures, maintains the perennial sea ice cover. Surface water salinity in the study area is about 31 [*Environmental Working Group*, 1997]. Below the surface flow, relatively warm (>0°C) and saline (34.75 or greater) modified Atlantic Water flows as a boundary current anticlockwise around the Arctic Ocean continental margin (Figure 1). The Atlantic Water enters the Arctic Ocean either across the Barents Sea shelf or as a branch of the West Spitsbergen Current [*Aagard et al.*, 1985; *Rudels et al.*, 1991, 1994, 1999]. Branches leave the continental slope along bathymetric features such as the Lomonosov Ridge, the Alpha-Mendeleev Ridge and the Gakkel Ridge, and form loops in the subbasins of the Arctic Ocean. In the Amerasian Basin and the outflow region of the Eurasian Basin, the water column above this Atlantic-derived layer contains the Pacific Water that enters via the shallow Bering Strait (40–50 m). The Pacific Water layer is characterized by relatively low salinity (<33) and a high nutrient content. The Eurasian and Amerasian Basins of the Arctic Ocean are separated by the Lomonosov Ridge with a sill depth of about 1500 m; as a result their deep waters have somewhat different properties.

[8] Seismic single channel reflection measurements were carried out parallel to coring along the drift of the GreenICE station [*Kristoffersen and Mikkelsen*, 2006]. The seismic results show that the top of southern Lomonosov Ridge is bevelled (550 m water depth) and only thin sediments (< 50 ms ~ 45 m ± 5 m) cover acoustic basement. About 1 km of sediments is found at the western entrance to the deep passage between southern Lomonosov Ridge and the Lincoln Sea continental margin. Here, the uppermost part (+ 0.3 s thick ~ 255 m ± 15 m) of the section probably reflects increased sediment input during the Plio–Pleistocene [*Kristoffersen and Mikkelsen*, 2006]. The core sections presented in this study are from the deeper, western part of the transect (Figure 1).

[9] In addition to the GreenICE core material, we studied late Holocene surface sediment samples from radiocarbon-dated box cores from the central Lomonosov Ridge (PS2185-3 and PS2177-1) and a site adjacent to the Morris Jesup Rise north of Greenland (PS2195-4) (Figure 1). We expect that late Holocene sediments were not recovered in the GreenICE cores and the purpose was to determine the late Holocene planktic foraminifera assemblage in the fraction >63–125 μm at interior Arctic sites where only the

Figure 1. (a) Arctic Ocean bathymetry, major surface currents (white), subsurface Atlantic Water circulation system (red), location of GreenICE study area (square, with detailed map given in Figure 1b), and additionally surface sediment samples studied (PS2177-1, PS2185-3, and PS2195-4). Other core sites mentioned in text are also shown. LS, Lincoln Sea; LR, Lomonosov Ridge; MJR, Morris Jesup Rise; GR, Gakkel Ridge; AR, Alpha Ridge; MR, Mendeleev Ridge; NR, Northwind Ridge; WSC, West Spitsbergen Current. The map source is the International Bathymetric Chart of the Arctic Ocean (IBCAO). (b) Detailed bathymetric map showing the drift track of the GreenICE station and location of coring sites 10 and 11.

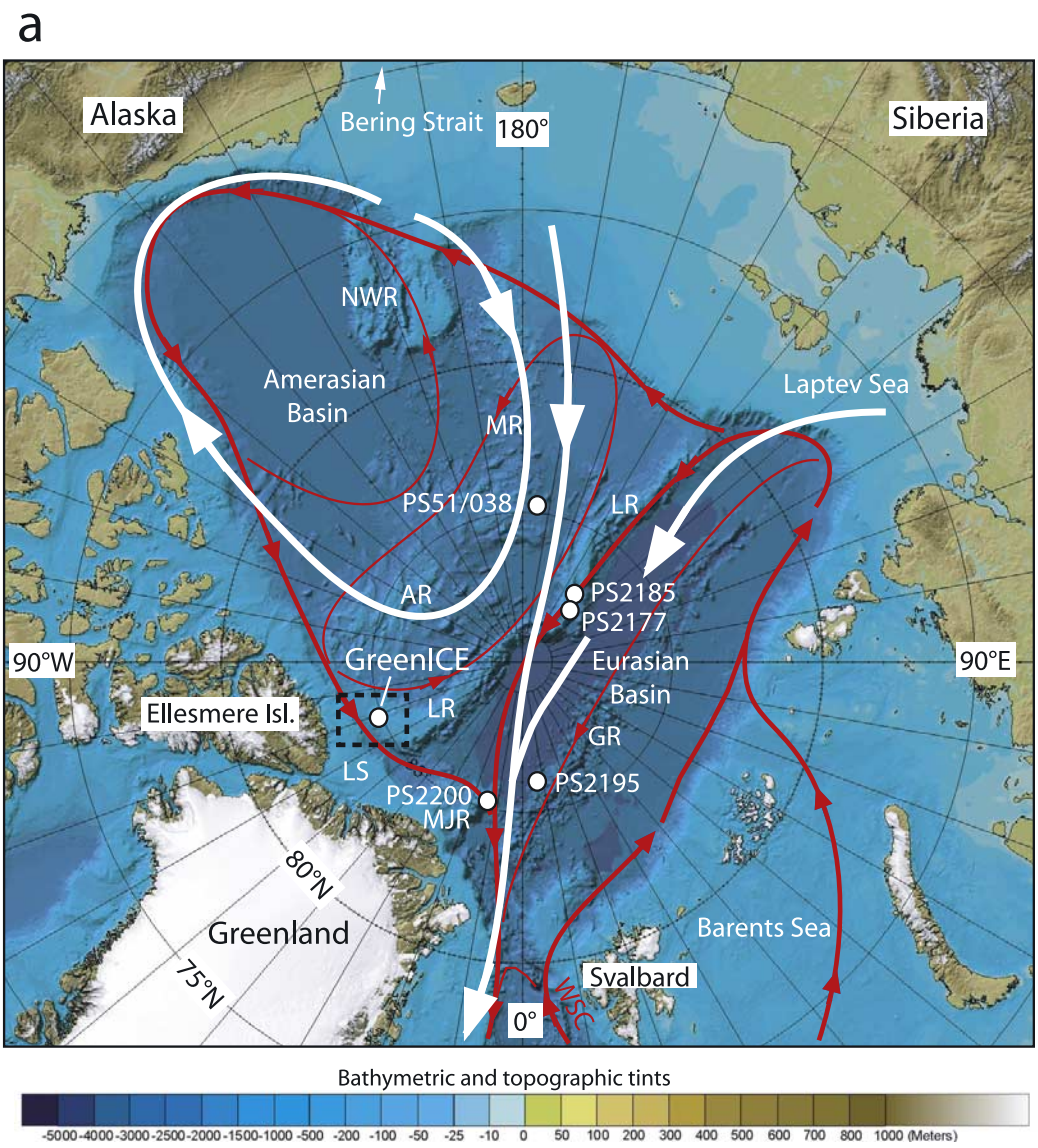
a
Alaska
Bering Strait
180°
Siberia
NWR
Amerasian Basin
MR
Laptev Sea
PS51/038
LR
AR
PS2185
PS2177
90°W
GreenICE
Eurasian Basin
90°E
Ellesmere Isl.
LR
GR
LS
PS2200
MJR
PS2195
80°N
Greenland
Barents Sea
75°N
Svalbard
0°
WSC
Bathymetric and topographic tints
-5000 -4000 -3000 -2500 -2000 -1500 -1000 -500 -200 -100 -50 -25 -10 0 50 100 200 300 400 500 600 700 800 1000 (Meters)
b
84°N
85°N
-80°
-75°
-70°
-65°
-60°
1500
1000
500
#11
#10

Figure 1

Table 1. GreenICE Coring and Surface Sediment Sampling Stations

Station Number	Latitude, °N	Longitude, °W	Water Depth, m	Sample Type	Core, length cm
1	84° 49.79	71°42.47	650	surface	-
2	84° 51.51	72° 08.91	691	surface	-
3	84° 51.40	72° 13.05	ca. 710	surface	-
4	84° 51.24	72° 19.79	730	surface	-
5	84° 50.23	72° 59.14	830	surface	-
6	84° 50.19	73° 07.25	845	core	10
7	84° 50.23	73° 17.05	902	core	24
8	84° 49.68	73° 51.42	1026	core (double penetration)	105
9	84° 49.58	73° 59.00	1006	surface	-
10	84° 48.76	74° 16.96	1040	core	176
11	84° 48.86	74° 15.75	1089	core	65
12	84° 48.16	75° 03.50	1117	surface	-
13	84°48.02	75° 10.50	1101	core	18
14	84° 47.90	75° 17.53	1086	surface	-
15	84° 47.61	75° 28.48	1071	core	22

fraction >125 μm hitherto has been investigated [*Nørgaard-Pedersen et al.*, 1998; *Hommers*, 1998].

3. Methods and Material

[10] A 2 m long gravity corer with 200 kg core head was suspended from a tripod and handled by a custom made hydraulic winch. The corer was fitted with a 25 cm long cone beneath the core catcher and a 9 cm inner diameter PVC core liner. Using a cone displaces the level upward at which the sediment column reaches the core catcher, thereby potentially enhancing the recovery of soft surface sediments. Several short gravity cores and surface samples were taken along the ice camp drift path between 650–1100 m water depth (Figure 1, Table 1). Core 10 and 11 recovered the longest sediment records of 176 cm and 65 cm, respectively. The shorter cores did not penetrate an IRD-rich, semilithified layer at about 20–40 cm subbottom depth.

[11] Shore-based laboratory work concentrated on detailed investigations of core 10 and 11. After splitting of the core sections, subsamples of 3–4 cm^3 were taken every 1–2 cm down core. The samples were wet-sieved (>63 μm, >1 mm) and the 63–1000 μm fraction was dry-sieved in subfractions (63–125 μm, 125–250 μm, 250–1000 μm). These samples were used for coarse fraction analysis, counting of ice-rafted debris (IRD) content, microfaunal analysis, and oxygen and carbon isotope measurements. Accelerator mass spectrometry (AMS) ^{14}C dating was carried out on ~10 mg samples of the planktic foraminifera *Neogloboquadrina pachyderma* (sinistral) at the Leibniz AMS laboratory, University of Kiel. Reservoir correction applied is −440 yr [*Mangerud and Gulliksen*, 1975]; however, actual reservoir time could be larger in the Arctic Ocean, especially during glacial periods [cf. *Voelker et al.*, 1998; *Haflidason et al.*, 2000]. In core 11, oxygen and carbon isotope measurements were carried out on planktic foraminifera *N. pachyderma* (s) from the 125–250 μm fraction (about 20 individuals per sample) at the Goodwin Laboratory, Cambridge. Nannofossil smear slides were prepared for selected sample intervals from cores 10 and 11 and examined using the light microscope. Owing to the scarcity of coccoliths in Arctic sediments, only about 50–100 specimens per sample were counted. Thus, as done by *Jakobsson et al.* [2000, 2001] and *Spielhagen et al.* [2004], occurrences of *Gephyrocapsa muellerae* and *Emiliana huxleyi* were primarily used to identify marine isotope stage (MIS) 5.

[12] The total planktic foraminifera abundance (specimens >63 μm/g) were determined on representative sample splits of the >63 μm size fraction from core 10 and 11 using a binocular microscope. In addition, planktic foraminifera species assemblages (>63 μm) were determined on core 11. Between 300 and 400 individuals per sample were identified. Previous studies of Arctic Ocean late Quaternary records, have traditionally studied specimens >150 μm or >125 μm, and found a planktic foraminifera assemblage totally dominated by the polar species *N. pachyderma* (s) with only subordinate occurrences of subpolar species *N. pachyderma* (dextral) and *Turborotalita*(= *Globigerina*) *quinqueloba* [*Foley and Poore*, 1993; *Nørgaard-Pedersen et al.*, 1998; *Hommers*, 1998; *Bauch*, 1999]. Studies of both living and fossil assemblages in the subpolar and marginal Arctic Ocean indicate, however, that valuable information are lost by neglecting the small size fraction [*Bauch*, 1994; *Hebbeln et al.*, 1994; *Dokken and Hald*, 1996; *Carstens and Wefer*, 1992; *Carstens et al.*, 1997; *Hald et al.*, 2004; *Volkmann*, 2000a, 2000b].

[13] Ice-rafted debris (IRD) grains >250 μm were counted on representative sample splits of core 11 and IRD grains/g were quantified. Moreover, in core 10 and 11 the downcore occurrence of IRD clasts with a diameter >0.5 cm ("dropstones") was noted during core description and later subsampling of core sections. The fraction >250 μm was used also to quantify the abundance of larger specimens of benthic foraminifera *Cibicides wuellerstorfi* and *Bulimina aculeata*. *B. aculeata* occurs in high numbers in a narrow stratigraphic interval in several cores from the central and Amerasian Arctic Ocean taken at water depths between 1000 and 2000 m [*Poore et al.*, 1993; *Ishman et al.*, 1996; *Jakobsson et al.*, 2001; *Polyak et al.*, 2004]. This species is virtually absent from the Arctic Ocean today, enabling its peak in abundance to be a distinct biostratigraphic marker. Together with nannofossil assemblage data, *B. aculeata* can be used as a stratigraphic marker for late MIS 5 in Arctic Ocean records [cf. *Backman et al.*, 2004].

4. Results

4.1. Sediment Core Stratigraphy

[14] All seven cores recovered appear to correlate visually, which indicate they are representative for the regional, hemi-

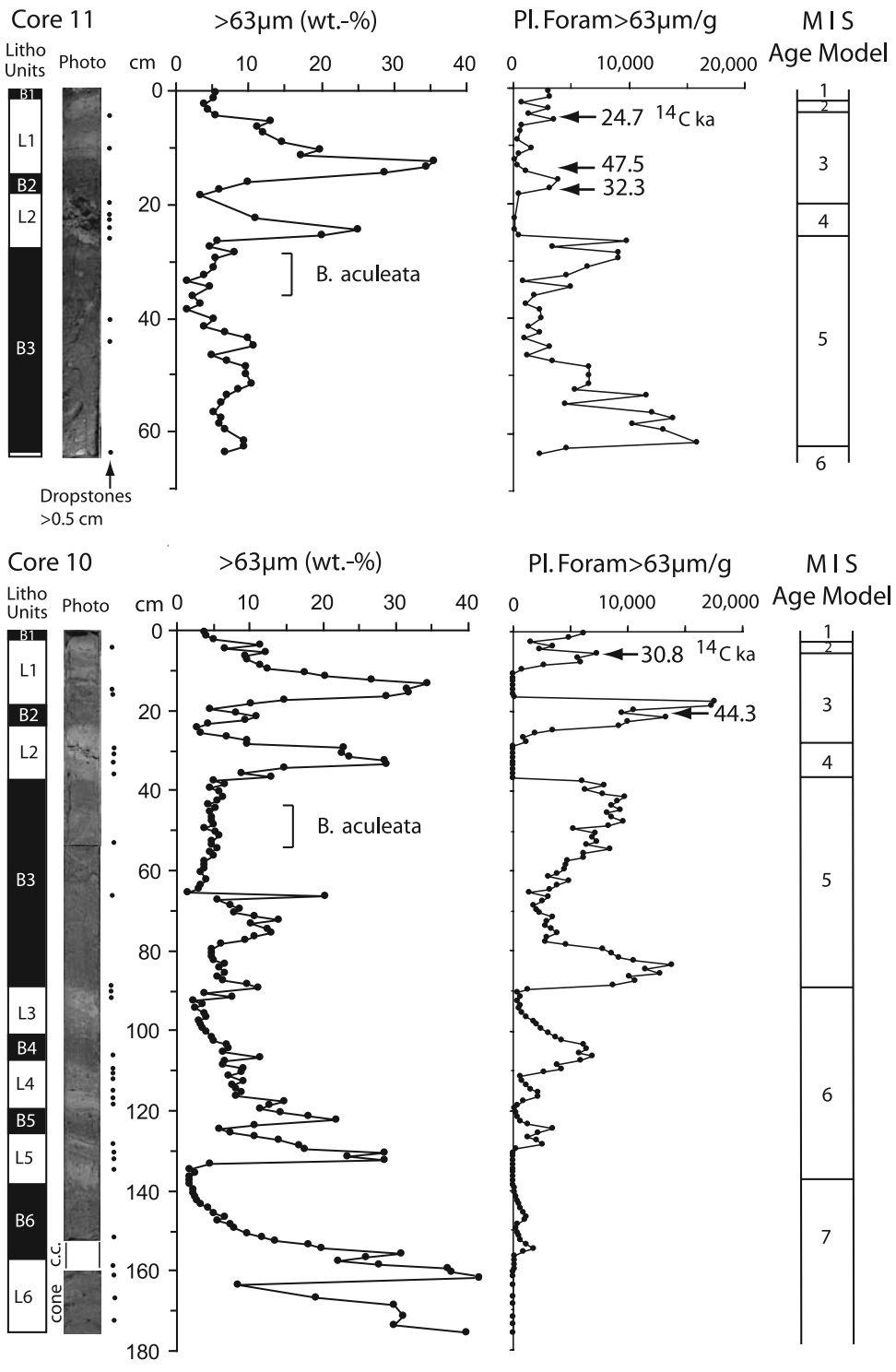

Figure 2. GreenICE cores 10 and 11, including core photos, lithounits, coarse fraction content >63 μm (wt-%), occurrence of "dropstones" >0.5 cm, planktic foraminifera abundance >63 μm, and age model (marine isotope stages (MIS) 1–7). The stratigraphic levels with AMS ^{14}C dates (^{14}C ka) and the peak occurrence of benthic foraminifera *Bulimina aculeata* are indicated. The sediment stratigraphy in the cone below the core catcher (c.c.) in core 10 was intact.

pelagic sediment succession in the area. The core sections consists of alternating dark brown (10 YR 6/3 and 10 YR 4/4) and light yellowish grey/brown (2.5Y 6/2 and 2.5Y 6/4) beds of clayey and sandy muds with occasional occurrence of dropstones, up to several cm in diameter (Figure 2). For descriptive purposes we will use a simplified lithostratigraphy counting "brown" (B) and "light-colored (L) beds from top to bottom. Brown beds are bioturbated silty clays which

Table 2. Accelerator Mass Spectrometry ^{14}C Dates of *N. pachyderma*(s) in GreenICE Cores 10 and 11[a]

Core Number	Depth, cm	Laboratory Identification	Delta ^{13}C	Conventional ^{14}C Age, yr BP	Reservoir-Corrected ^{14}C Age, kyr BP
GreenICE 10	5–6	KIA 25763	0.82 ± 0.04	31210 + 500/−470	30.8
GreenICE 10	18–19	KIA 25764	0.39 ± 0.14	44760 + 390/−380	44.3
GreenICE 11	5–6	KIA 25760	−0.06 ± 0.06	25170 + 240/−230	24.7
GreenICE 11	13–14	KIA 24847	−0.16 ± 0.30	47910 + 1540/−1290	47.5
GreenICE 11	17–18	KIA 25761	−2.06 ± 0.10	32690 + 600/−550	32.3

[a]Reservoir correction applied is -440 yr [*Mangerud and Gulliksen*, 1975].

are rich in calcareous microfossils such as planktic and benthic foraminifera and ostracods and commonly with nannofossils. Light-colored beds range from silty clays to sandy silts with occasional granule to small pebble-sized IRD and a sparse microfossil content. Preliminary data on bulk sediment $CaCO_3$ content show that the cores contain a relatively high background $CaCO_3$ content of 10–20% with peaks of $CaCO_3$ exceeding 30% in the fine-grained light-colored units. Unit L2 contains abundant semiconsolidated, fine-grained carbonate material.

[15] Calcareous planktic and benthic foraminifera, and late Quaternary nannofossils are very well preserved in core 10 and 11. This is also true for intervals showing low foraminifera abundances (typically with a high $CaCO_3$ content). The basal part of core 10 (below 165 cm), though, appears to be barren of calcareous specimens, and contains a sparse assemblage of agglutinated benthic foraminifera. The basal part also reveals a very low $CaCO_3$ content. Apart from the coarse fraction peaks at about 15 cm (lower part of L1) and about 130 cm (L5) subbottom depth showing sorting in the very fine sand mode and dark color banding (iron-manganese coating?), indications of current sorting/winnowing appear to be absent.

[16] The age models for core 10 and 11, described in detail below, are based on a combination of AMS ^{14}C dating from planktic foraminifera (Table 2), nannofossil assemblage stratigraphy (Table 3), and characteristic benthic foraminifera biostratigraphic markers. Furthermore, characteristic color changes and variable microfossil content have been used to correlate with radiocarbon-dated cores from the interior Arctic Ocean [*Darby et al.*, 1997; *Nørgaard-Pedersen et al.*, 1998] and mark transitions between marine isotope stages (MIS) 1–3. Because of the specific nature of the Arctic Ocean's upper surface structure, the isotopic record of *N. pachyderma* (s) (core 11) is only of limited stratigraphic help.

4.1.1. Core 11 Age Model

[17] At 5–6 cm, an AMS ^{14}C date of 24.7 ^{14}C kyr BP was obtained (Table 2). Accordingly, the light brownish grey, fine-grained layer from 5–2 cm (L1) corresponds to peak glacial MIS 2 (24–12 ka), based on correlation with central Arctic records [*Darby et al.*, 1997; *Nørgaard-Pedersen et al.*, 1998, 2003]. The topmost dark brown sediment (B1) is of Holocene age, on the basis of its elevated content of planktic foraminifera, benthic foraminifera *C. wuellerstorfi*, and nannofossils including *E. huxleyi, G. muellerae, C. pelagicus*, and *G. carribeanica* (Figure 3, Table 3). We suspect, though, that the younger part of the Holocene record was lost during the coring process. The two dates at 13–14 cm (sandy lower part of L1: 47.5 ^{14}C kyr BP) and 17–18 cm (B2: 32.3 ^{14}C kyr BP) reveal an age reversal. The corresponding B2 unit in core 10 gave an AMS ^{14}C age of 44.3 ^{14}C kyr BP. The influence of very low sedimentation rate, bioturbation and larger uncertainty of AMS dates close to the dating limit (about 50 kyr BP), possible can explain the scatter of ages obtained. From interior Arctic Ocean box cores, ages of 50–30 ^{14}C kyr have been obtained in a similar foraminifera-rich brown unit [*Darby et al.*, 1997; *Nørgaard-Pedersen et al.*, 1998]. On the basis of stratigraphic evidence from the bounding units, the IRD-rich unit from 26–20 cm (L2) probably represents MIS 4 to early MIS 3. The thick brown B3 section contains common calcareous nannofossils dominated by *G. muellerae* (80–90%) with subordinate *E. huxleyi*, and occasionally, *G. oceanica*, *G. carribeanica,* and *C. pelagicus* (Figure 3, Table 3). From this section upward to the nannofossil-bearing units in B2-B1, there is a clear shift toward a decrease in *G. muellerae* (20–60%) and a marked increase in *E. huxleyi* (30–80%). This corresponds with the transition seen between the MIS 5/4 transition (74 ka) and MIS 4/3 (59 ka) in the nannofossil biozonation scheme for high northern latitudes [*Gard*, 1988; *Gard and Backman*, 1990]. The validity of the aforementioned scheme for interior Arctic records was recently demonstrated by *Jakobsson et al.* [2000, 2003], *Spielhagen et al.* [2004], and *Backman et al.* [2004]. Furthermore, abundance peaks of the benthic foraminifera *B. aculeata* at 30–28 cm supports that this stratigraphic level corresponds to late MIS 5 [cf. *Backman et al.*, 2004; *Polyak et al.*, 2004]. Considering that the interval from 62–53 cm reveals a prominent peak in subpolar planktic foraminifera and *C. wuellerstorfi* (Figures 3 and 4), this level is assigned to the last interglacial (substage 5e). On basis of correlation to core 10 (Figure 2, see below also), it is suggested that the lowermost trend in the core 11 record, demonstrating a sharp reduction downward in total planktic foraminifera/g sediment, percentage subpolar foraminifera and nannofossil content, represents the transition to the penultimate glacial period (MIS 6).

4.1.2. Core 10 Age Model

[18] The lithostratigraphic and biostratigraphic data of core 10 (Figure 2, Table 3) indicate that the record of the upper 90 cm in detail can be correlated to the record of core 11, encompassing MIS 5-1. Two AMS ^{14}C dates at 5–6 cm (L1: 30.8 ^{14}C kyr BP) and 18–19 cm (B2: 44.3 ^{14}C kyr BP) corroborate the stratigraphic framework of MIS 3-1 sediments. Like in core 11, the nannofossil data reveal that the thick brown B3 unit is dominated by *G. muellerae* with subordinate *E. huxleyi*, supporting a MIS 5 age. Occasional occurrences of *G. oceanica*, *G. carribeanica,* and

Table 3. Results of Nannofossil Analysis of Selected Samples From Different Litho-units in GreenICE Cores 11 and 10[a]

Depth, cm/Unit	*G. muellerae*	*E. huxleyi*	*G. oceanica*	*G. caribbeanica*	*C. pelagicus*	Remarks
			GreenICE Core 11			
0.0/B1	X	X	-	X	x	
1.5/B1-L1	-	-	-	-	-	barren
4.5/L1	-	-	-	-	-	barren
5.5/L1	X	X	-	x	x	
7.5/L1	-	-	-	-	-	barren
12.5/L1	-	-	-	-	-	barren
14.5/L1	-	-	-	-	-	barren
16.0/B2	X	X	-	-	-	
17.5/B2	X	X	x	-	-	
20.5/L2	-	-	-	-	-	barren
23.5/L2	-	-	-	-	-	barren
32.0/B3	X	x	x	x	-	
40.0/B3	X	x	x	x	-	
46.0/B3	X	x	-	x	-	
55.0/B3	X	X	x	-	-	
58.5/B3	X	X	-	-	x	
60.5/B3	X	x	x	-	x	
64.0/B3-L3	-	-	-	-	-	barren
			GreenICE Core 10			
7.5/L1	X	X	x	x	-	
14.5/L1	-	-	-	-	-	barren
20.5/B2	X	X	-	x	-	
26.5/L2	x	-	-	x	-	rare
32.5/L2	-	-	-	-	-	barren
39.5/B3	X	X	X	x	x	
49.5/B3	X	-	x	X	-	
59.5/B3	X	x	x	x	x	
67.5/B3	X	x	-	x	-	
74.5/B3	X	X	-	x	-	
79.5/B3	X	X	-	x	-	
84.5/B3	X	X	-	-	-	
87.5/B3	X	X	x	x	x	
91.5/L3	-	-	-	-	-	barren
99.5/L3	-	-	-	-	-	barren
104.5/B4	X	X	x	x	-	
112.5/L4	x	-	-	-	-	rare
119.5/L4	x	-	-	-	-	rare
124.5/B5	X	X	x	x	-	
129.5/L5	x	-	-	-	-	rare
136.5/L5	x	-	-	-	-	rare
144.5/B6	X	X	x	x	-	
151.5/B6	X	X	x	-	-	

[a]The results are given as follows: X, occurrence; x, rare occurrence; -, no occurrence.

C. pelagicus appear to be most common in the upper and lower part of B3. An abundance peak of *B. aculeata* at 54–53 cm supports the finding in core 11, and a MIS 5a age is assigned to the upper part of unit B3. Similar to core 11, the lower part of B3 is characterized by an abundance peak of planktic foraminifera (including subpolar specimens), and likewise, this stratigraphic interval is assigned to the last interglacial (substage 5e). As the light-colored units between 140–90 cm (L5-L3) are enriched in IRD supporting dominantly glacial conditions, this section is tentatively assigned to MIS 6. The thicker brown unit (B6) below (160–140 cm) contains only a moderate number of planktic and benthic foraminifera and nannofossils. However, *Pullenia* sp. benthic foraminifera found in this unit, support that this unit may correspond to the penultimate interglacial MIS 7. Thus other studies indicate that *Pullenia* sp. benthic foraminifers appear to occur exclusively in the MIS 7 interval in Amerasian Basin and central Lomonosov Ridge cores [*Jakobsson et al.*, 2001; *Backman et al.*, 2004]. The basal part of core 10 (L6) also reveal a transition upward from agglutinated benthic foraminifers only to calcareous specimens. A similar faunal transition is well-known from a number of Arctic Ocean records [*Poore et al.*, 1993, 1999; *Jakobsson et al.*, 2001; *Backman et al.*, 2004]. For central Lomonosov Ridge records, *Backman et al.* [2004] infer that the agglutinated/calcareous faunal transition is close to the MIS 8/7 boundary, but may be diachronous with up to 50 kyr between the central Arctic Ocean and Northwind Ridge sites. Moreover, as coccolith species *Emiliana huxleyi* are found in unit B6, it can be inferred that the basal sediment recovered is probably younger than (or equal to) late MIS 8, as its first evolutionary appearance is dated to about 0.26 Ma [*Thierstein et al.*, 1977].

4.2. Foraminifera Record

[19] In general, high planktic foraminifera (>63 μm) abundances are found in the dark brown lithounits (2000–15000 specimens/g) and very low abundances are found in the

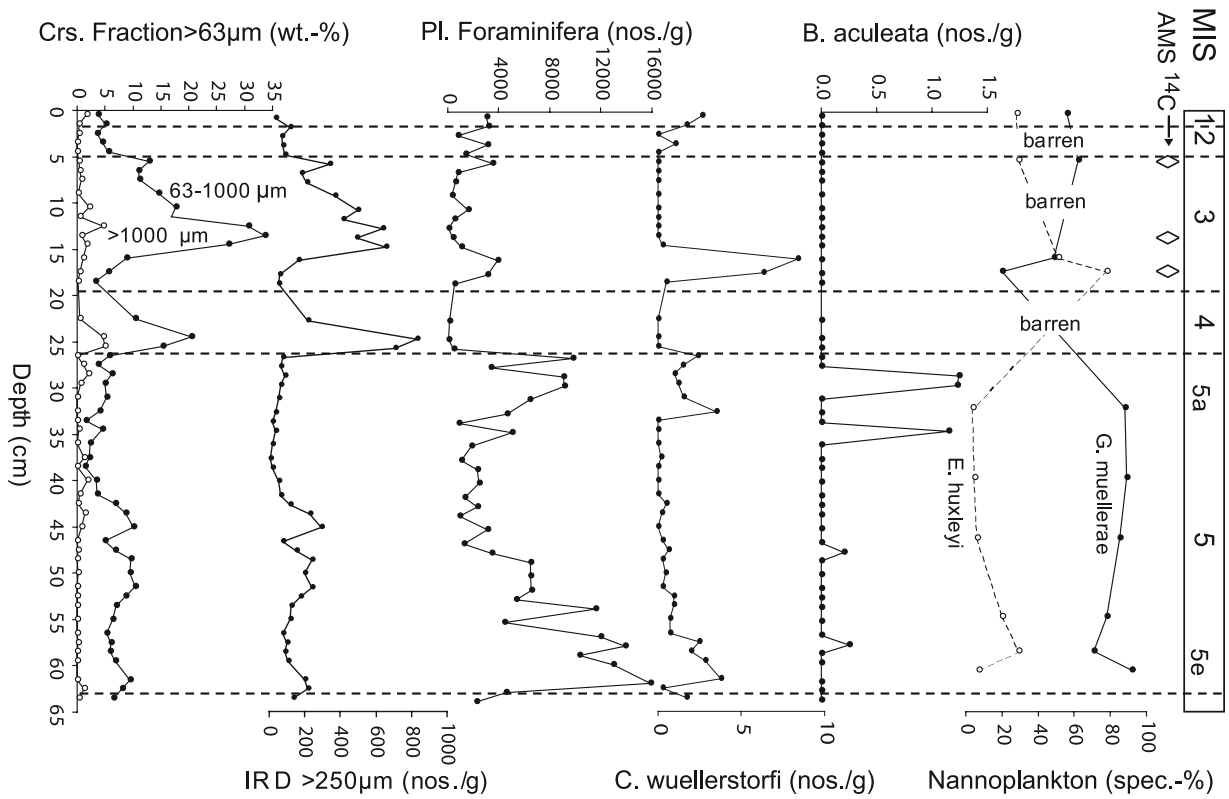

Figure 3. Basic stratigraphic data of core 11, including coarse fraction content >63 μm (wt-%), IRD>250 μm (grains/g), planktic foraminifera abundance (specimens >63 μm/g), selected benthic foraminifera *C. wuellerstorfi* and *B. aculeata* (specimens >250 μm/g), and nannofossil assemblage: E. huxleyi and G. muellerae (percentage of total assemblage). Marine isotope stage (MIS) age model with substages 5e (last interglacial) and 5a (warm interstadial) is shown to the right.

light-colored units (<1000 specimens/g) (Figures 2 and 3). The core top sediments (B1) contain about 5000 specimens/g. The lower and upper part of unit B3 (assigned to MIS substages 5e and 5a) show in both core 10 and 11 peak abundances (8000–15000 specimens/g) of planktic foraminifera. The dark brown units below (B4-B6) contain a more moderate amount of planktic foraminifera (2000–5000 specimens/gram). The preservation of the planktic foraminifera tests is excellent even at transitions between units rich in foraminifera and units poor in foraminifera. Intervals barren of planktic foraminifera are found only in unit L2 (29–34 cm), L5 (130–134 cm), and the lowermost part of core 10 (below 165 cm).

[20] Planktic foraminifera species assemblages >63 μm have been quantified only in core 11 (MIS 1-5), but microscopic investigations of core 10 samples (MIS 1-5) reveal no major difference in the composition of assemblages between the two cores. The assemblages are in general dominated by *Neogloboquadrina pachyderma* (sinistral). In specific intervals, however, small subpolar *Turborotalita quinqueloba*(= *Globigerina quinqueloba*) comprise a significant part of the assemblage (20–50%). *Neogloboquadrina pachyderma* (dextral) are found throughout the core (3–15%), but do not appear to show any significant covariation with other parameters. Other species like *Globigerina glutinata* and *Globigerina bulloides* occur rarely.

[21] Small *T. quinqueloba* (63–125 μm) are particularly abundant in two intervals also revealing peak abundances in planktic foraminifera; the lower and upper part of unit B3 assigned to MIS 5 (Figure 4). The lower abundance peak representing substage 5e (last interglacial) reveals approximately 40–50% *T. quinqueloba*, whereas the upper peak representing substage 5a contains 20–35% *T. quinqueloba*. The upper part of core 11 assigned to MIS 3-1 contains a relatively unimodal planktic foraminifera assemblage with $\geq$90% *N. pachyderma* (s), 5–10% *N. pachyderma* (d), and <5% *T. quinqueloba*. The core top sediment samples from the GreenICE sites contain a planktic foraminifera assemblage (>63 μm) totally dominated by *N. pachyderma* (s). *T. quinqueloba* occur very rarely (1%) and *N. pachyderma* (d) make up 10% or less (Table 4).

[22] The late Holocene surface sediment samples (>63 μm) from central Lomonosov Ridge box cores (PS2177-1, PS2185-3) and a site in the Amundsen Basin adjacent to Morris Jesup Rise (PS2195-4) (Figure 1) reveal a similar pattern, with a clear *N. pachyderma* (s) dominance (91–95%), and with *T. quinqueloba* only comprising about 1% of the assemblage (Table 4). AMS ^{14}C dates of these surface sediment samples are in the range 2.5–3.2 ^{14}C kyr BP [*Nørgaard-Pedersen et al.*, 1998], which is typical for interior Arctic Ocean sites characterized by hemipelagic sedimentation [cf. *Stein et al.*, 1994; *Darby et al.*, 1997].

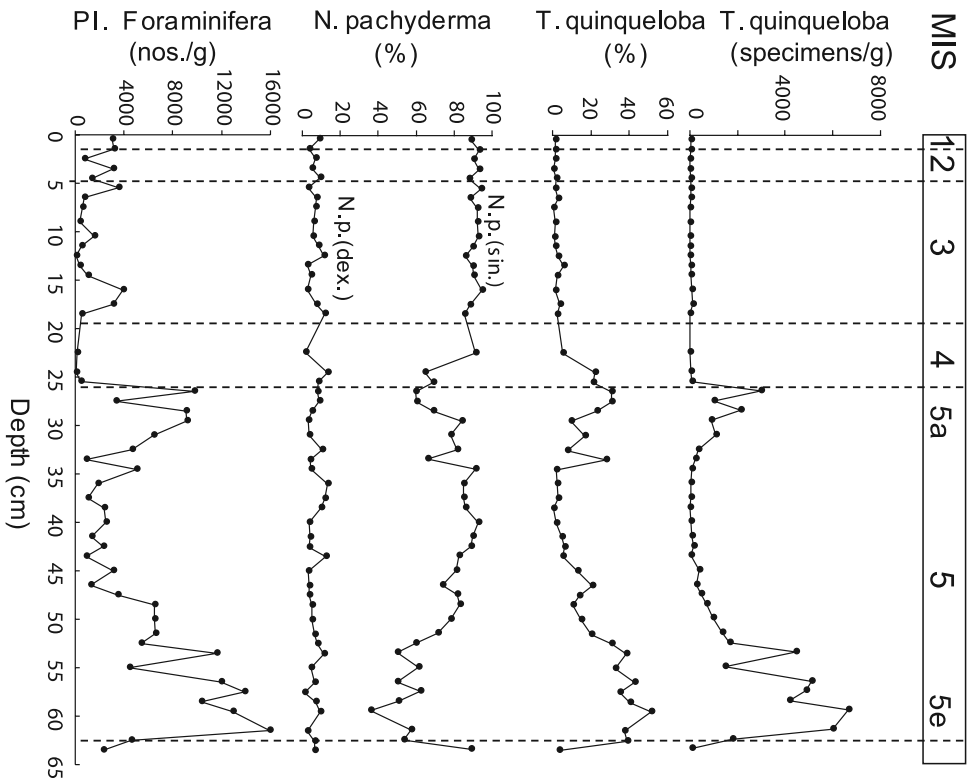

Figure 4. Core 11 planktic foraminifera assemblage record (specimens >63 μm). The two intervals assigned to substages 5e and 5a are characterized by abundant subpolar foraminifera *T. quinqueloba*, whereas polar species *N. pachyderma* (s) dominate totally in the other part of the record.

[23] Quantification of benthic foraminifera *Cibicidoides wuellerstorfi* and *Bulimina aculeata* in core 11 reveal that moderately high numbers of *C. wuellerstorfi* occur in the intervals assigned to MIS 5e, 5a (unit B3), mid MIS 3 (unit B2), and the Holocene (unit B1) (Figure 3). Abundant *B. aculeata* are observed in core 11 in the 35–28 cm interval (upper part of unit B3) with only few specimens found below (57–56 cm and 47–46 cm) (Figure 2). A similar abundance peak of *B. aculeata* is seen in the adjacent core 10, in the correlative level 57–53 cm with a scattered occurrence only down to 67 cm.

4.3. δ^{18}O and δ^{13}C Data

[24] The δ^{18}O and δ^{13}C record (*N. pachyderma* (s)) of core 11 (Figure 5) exhibits significant variability as we might expect for an interior Arctic Ocean site where the global ice-volume glacial-interglacial pattern [cf. *Lea et al.*, 2002] is masked by the influence of surface water salinity changes [*Spielhagen and Erlenkeuser*, 1994; *Nørgaard-Pedersen et al.*, 1998; *Polyak et al.*, 2004; *Spielhagen et al.*, 2004]. Relatively low δ^{18}O values (1.0–2.0 ‰) associated with low δ^{13}C values are observed in the record of early to mid MIS 5. Intervals of very high δ^{18}O values (2.5–3.5 ‰) and relatively high δ^{13}C values characterize the midstage 5 to MIS 4 record. In uppermost MIS 5 sediments, however, a brief incursion of low δ^{18}O/low δ^{13}C is seen. The MIS 3-1 record exhibits relatively low δ^{18}O values (1.0–2.0 ‰) associated with low δ^{13}C values, but the low resolution may preclude detection of isotopic changes related to the last glacial-interglacial transition. The core top δ^{18}O value of about 1.3 ‰ is close to average values obtained from other Holocene records from the

Table 4. Planktic Foraminifera Species Assemblages >63 μm in Core Top Samples From GreenICE Cores 10 and 11 Compared to Late Holocene Surface Sediment Samples From Cores PS2177-1 and PS2185-3 in the Central Lomonosov Ridge and Core PS2195-4 in the Amundsen Basin[a]

Core Number	*N. pachyderma,* (sin) %	*N. pachyderma,* (dex) %	*T. quinqueloba,* %	Indeterminata, %
GreenICE 10	90.4	7.2	1.0	1.4
GreenICE 11	89.0	9.1	1.3	0.6
PS2177-1	91.8	5.5	1.2	1.5
PS2185-3	95.1	3.4	0.5	1.0
PS2195-4	95.5	3.1	0.7	0.7

[a]See Figure 1 for location.

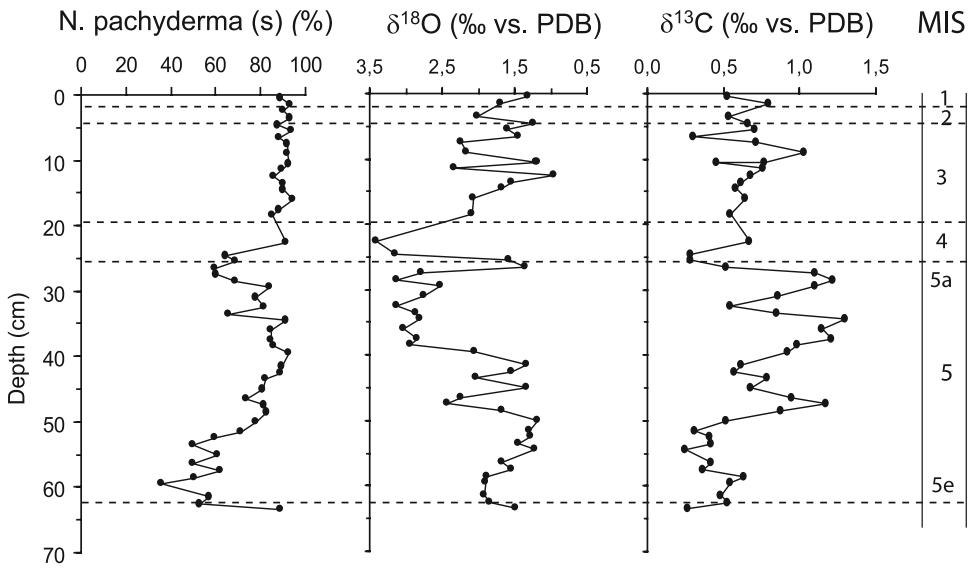

Figure 5. Core 11 oxygen and carbon isotope record (*N. pachyderma* (s)). For comparison, the *N. pachyderma* (s) content (%) is shown also. Marine isotope stage (MIS) age model with substages 5e (last interglacial) and 5a (warm interstadial) is shown to the right.

Amerasian basin [*Poore et al.*, 1999; *de Vernal and Hillaire-Marcel*, 2005] and the central Lomonosov Ridge [*Nørgaard-Pedersen et al.*, 1998, 2003].

4.4. IRD Record

[25] From the quantification of IRD>250 μm in core 11, it is evident that the peaks in coarse fraction (>63 μm) content (including biogenic remains and authigenic aggregates) parallel peaks in the IRD content (Figure 3). On the basis of this and the occurrence pattern of dropstones >0.5 cm (Figure 2), intervals of increased IRD content can be inferred also for core 10. Peak values of 500–2000 grains >250 μm/g are found in the units assigned to MIS 6, 4, and late MIS 3. However, it is possible that the IRD concentration in the late MIS 3 unit has been influenced by current winnowing, as noted. The lower middle part of unit B3 (?substage 5d) contains an elevated IRD content (200–300 grains/g). Light microscopic investigation of the >1000 μm grain lithology in both cores indicates a relatively uniform IRD composition throughout most of the record. Quartz, detrital carbonate, sandstone, and metamorphic rock fragments are the most abundant lithologies. Small pebbles of dark grey carbonate rock are common in the MIS 4 unit, also containing abundant semiconsolidated, fine-grained carbonate material. Noteworthy, the basal part of core 10 show IRD enriched in quartz with almost no detrital carbonate.

5. Discussion

5.1. Age Model

[26] The nannofossil assemblage combined with benthic foraminifera stratigraphic markers reveal that GreenICE core 11 (65 cm long) encompasses a record of MIS 5-1. Core 10 (176 cm long), which show a MIS 5-1 record very similar to core 11, probably reaches into MIS 7 or late MIS 8 sediments. Importantly, the lowermost part of core 10 (below 165 cm) appears to contain the agglutinated/calcareous faunal transition known from many sites in the Arctic Ocean [*Backman et al.*, 2004].

[27] The established age models for cores 11 and 10 imply that sedimentation rates for the GreenICE site are in the range 0.5–1.0 cm/kyr for the last two glacial-interglacial cycles. This is about half the rate determined for sites on the central part of the Lomonosov Ridge [cf. *Backman et al.*, 2004, and references therein]. In the discussion on late Quaternary Arctic Ocean sedimentation rates, it is important to note that the central Arctic and Eurasian Basin occurrence of relatively thick (0.5 m or more) sandy units (quartz-rich and poor in bulk $CaCO_3$ content [cf. *Backman et al.*, 2004; *Spielhagen et al.*, 2004]) results in considerably increased bulk sedimentation rates for these sites (Figure 6). In most Amerasian basin sites, these characteristic sandy units are absent or can be observed to thin out away from the central Lomonosov and Alpha-Mendeleev Ridge [cf. *Minicucci and Clark*, 1983; *Phillips and Grantz*, 2001; *Polyak et al.*, 2004]. At the GreenICE site, sedimentation rates for the MIS 5 interval appear to have been in the range 0.8–1.0 cm/kyr; almost twice the rate obtained for the MIS 4-2 interval (0.4–0.5 cm/kyr), dominated by glacial conditions. The youngest Holocene deposits were probably lost during the coring process, so we cannot make an estimate of recent sedimentation rates.

5.2. Planktic Foraminiferal Stratigraphy

[28] In GreenICE cores 10 and 11, abundant well-preserved calcareous planktic and benthic foraminifera are found in specific intervals of interglacial MIS 7, 5, and 1, as well as some interstadials of MIS 3 and 6. Correlatable planktic foraminifera-rich units are found in other interior Arctic sediment cores (Figure 6). The association of the foraminifera peaks with dark brown, fine-grained mud poor in IRD supports oxygenated bottom water conditions,

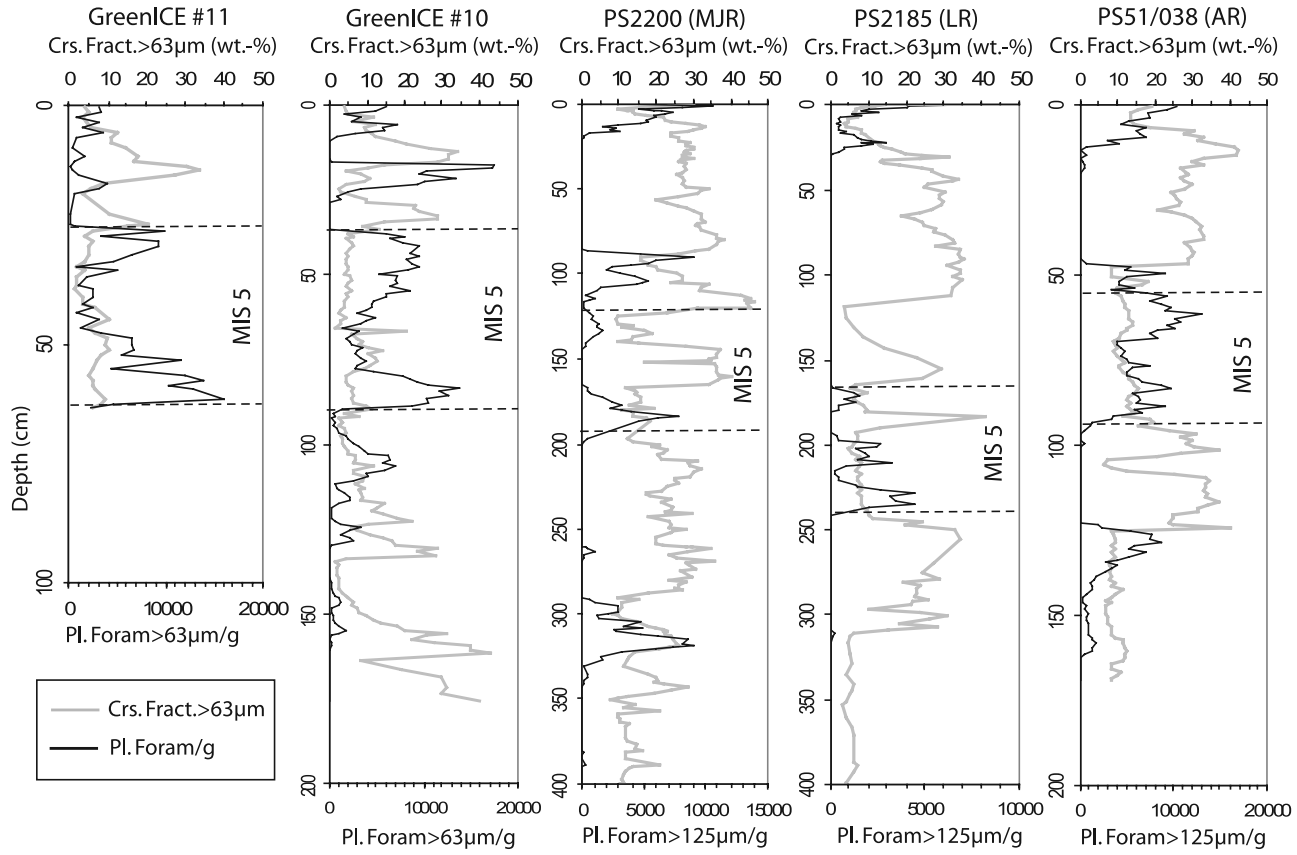

Figure 6. Comparison of coarse fraction content (grey line) and planktic foraminifera abundance (black line) in GreenICE cores 11 and 10, Morris Jesup Rise core (PS2200), Lomonosov Ridge core PS2185, and Alpha Ridge core PS51/038 (location indicated on Figure 1). Data from the latter three sites (including MIS 5 interval) are from *Spielhagen et al.* [2004].

dominant sea ice sediment rafting, open water leads during summer, and moderate high planktic productivity [*Poore et al.*, 1993; *Phillips and Grantz*, 1997; *Nørgaard-Pedersen et al.*, 1998; *Jakobsson et al.*, 2000; *Polyak et al.*, 2004]. The very simplified interpretation of interglacial sediment facies in the GreenICE cores has been refined by a detailed study of the planktic foraminifera assemblages. The very good preservation state of the planktic foraminifera throughout the cores (except basal part of core 10), and the high bulk sediment $CaCO_3$ content, support that the foraminifera assemblages have not been biased seriously by carbonate dissolution. We find remarkably high abundances of subpolar planktic foraminifera *T. quinqueloba* (>63 μm) in two sections, most likely representing substages 5e (last interglacial) and 5a (warm interstadial). The planktic foraminifera peaks dated to mid-MIS 3 and the Holocene, on the other hand, reveal planktic foraminifera assemblages (>63 μm) totally dominated by polar *N. pachyderma* (s). Late Holocene surface sediment samples (>63 μm) from additionally studied interior Arctic Ocean sites also show a clear dominance of *N. pachyderma* (s).

[29] The discovery of abundant subpolar *T. quinqueloba* in interior Arctic Ocean late Quaternary records is new. Usually larger size fractions (>125 μm or >150 μm) have been studied and a total dominance of polar foraminifera *N. pachyderma* (s) with subordinate *N. pachyderma* (d) has been reported for late Quaternary records [e.g., *Poore et al.*, 1993; *Hommers*, 1998; *Polyak et al.*, 2004]. A few studies, however, mention species assemblages in the finer fraction 63–125 μm, but with a scarce content of *T. quinqueloba* only [e.g., *Poore et al.*, 1993; *Backman et al.*, 2004]. Studies investigating the <150 μm fine fraction in the subpolar to temperate Nordic Seas, have revealed that *T. quinqueloba*, that is dominant during peak interglaciations, seems to become reduced in size under a cooler temperature regime [*Bauch*, 1994]. Persistence of these smaller *T. quinqueloba* in the Nordic Seas and the Fram Strait during interstadial periods and certain glacial stadials, allows relatively warm Atlantic Water advection to this region to be traced during periods other than peak interglaciations [*Hebbeln et al.*, 1994; *Dokken and Hald*, 1996; *Bauch et al.*, 2001; *Kandiano and Bauch*, 2002].

[30] At present, *T. quinqueloba* shows maximum abundance in the Nordic seas along oceanic fronts, in particular the Arctic Front that separates Atlantic and Arctic Water masses [*Johannesen et al.*, 1994]. Although the ecological preferences of this species are not yet clear, it has been suggested that in the Nordic seas it is a proxy for Atlantic water input [*Kandiano and Bauch*, 2002]. The Fram Strait and the southwestern Eurasian Basin, currently characterized by strong subsurface advection of Atlantic water below colder and lower-salinity polar surface water, contain abun-

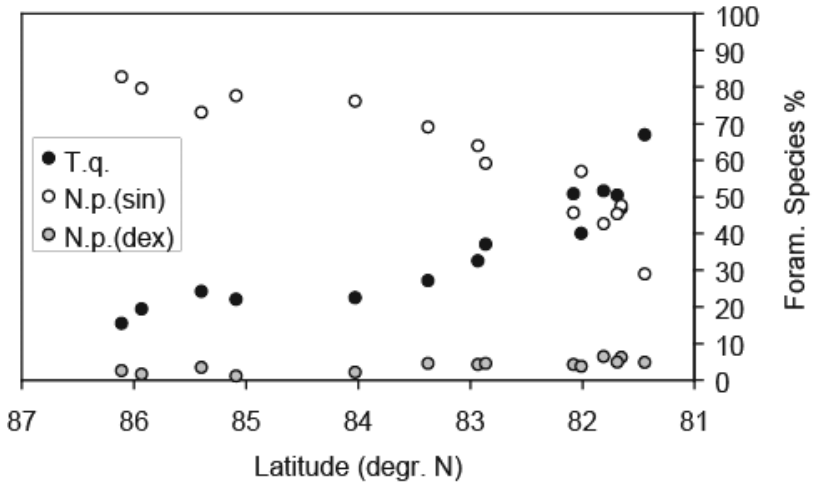

Figure 7. Recent distribution of planktic foraminifera (species >63 μm) in the upper 500 m water column of the Nansen Basin along a S-N transect from the northern Barents Sea margin (81°N) to the Gakkel Ridge (86°N). Subpolar species *T. quinqueloba* are found abundantly in the southern region characterized by strong advection of Atlantic Water. Data are from *Carstens and Wefer* [1992].

dant small subpolar *T. quinqueloba* in the water column [*Carstens and Wefer*, 1992; *Carstens et al.*, 1997; *Volkmann*, 2000a, 2000b]. The abundance of *T. quinqueloba* declines steadily further to the north (Figure 7). Despite the high abundance of *T. quinqueloba* in the water column, sediment surface samples along the Barents Sea margin and the adjacent deep Arctic Ocean show an assemblage totally dominated by *N. pachyderma* (s) [*Volkmann*, 2000b]. This is explained by selective dissolution of the subpolar *T. quinqueloba* by corrosive shelf-derived waters [*Aagard et al.*, 1985; *Steinsund and Hald*, 1994; *Volkmann*, 2000b]. Accordingly, many Holocene and last interglacial sections in that region appear to be severely influenced by carbonate dissolution [*Knies et al.*, 2000; *Wollenburg et al.*, 2001; *Matthiessen et al.*, 2001].

[31] The oxygen and carbon isotope data (*N. pachyderma* (s)) from GreenICE core 11 do not appear to reveal changes in the surface ocean salinity and ventilation rate covarying with the planktic foraminifera species changes within MIS 5. The sudden increases of δ^{18}O values within MIS 5 with up to 1 ‰ are well above the values that can be explained by global δ^{18}O-water changes. It implies a remarkable increase in surface water salinity at the site. Similar trends have been reported in δ^{18}O records from Mendeleev Ridge [*Polyak et al.*, 2004], Alpha Ridge [*Scott et al.*, 1989], central Lomonosov Ridge, and Morris Jesup Rise [*Spielhagen et al.*, 2004]. *Polyak et al.* [2004] suggested that the maxima of δ^{18}O values occurring in some interstadials could be due to the cessation of low-salinity Pacific Water inflow, when the Bering Strait was closed owing to global sea level fall. The present sill depth of the Bering Strait is about 40–50 m, and critical reductions of sea level during the last interglacial-glacial cycle were reached in MIS substages 5d, 5b, and stage 4-2 [cf. *Lea et al.*, 2002].

5.3. Paleoceanography and Sea Ice

[32] The discovery of a large numbers of small *T. quinqueloba* in the early and late MIS 5 record at the GreenICE site indicates paleoceanographic conditions in the area different from today. At Present, the area is heavily ice-covered and remote from sea ice margins and polar *N. pachyderma*(s) totally dominate the planktic foraminifera assemblage in surface sediments. Could this imply that advection of Atlantic Water to the interior Arctic Ocean was much stronger during the last interglacial MIS 5e and warm interstadial MIS 5a? Or was the sea ice margin placed further to the north so that the GreenICE site was situated at an ice-marginal or periodically ice-free position? Nordic Sea studies have shown that, when exclusively small sized specimens of *T. quinqueloba* are found, there is most likely a relation to advection processes [*Kandiano and Bauch*, 2002]. Indeed, a submerged Atlantic Water layer, below an ice-covered halocline can also carry and transport abundant numbers of subpolar foraminifera some distance into the Arctic Ocean. However, the consistent reduction of subpolar specimen abundances in the downstream, mostly ice-covered areas of the two Atlantic Water inflow branches (Spitsbergen Current and Barents Sea Current) indicate that present-day oceanographic circulation cannot explain the high *T. quinqueloba* abundancy during MIS 5 warm periods. Thus the percentage of *T. quinqueloba* are reduced from ≥50% in the Barents Sea Branch to <10% along the Laptev Sea margin [*Volkmann*, 2000a]. From the northern Barents Sea margin (influenced by the core of the West Spitsbergen Current) abundancies of *T. quinqueloba* ≥50% are reduced to less than 20% over the Gakkel Ridge at 86°N (Figure 7) [*Carstens and Wefer*, 1992]. Subpolar foraminifera carried to the GreenICE site via the present-day subsurface Atlantic Water boundary current (from high productive ice margin or ice free sites like the Fram Strait) would have to travel several thousands kilometers and probably only traces of an original assemblage would arrive at the destination (see Figure 1). Therefore we envisage for the early and late MIS 5 that high productive regions, probably with a reduced sea ice cover, were situated relatively near to the GreenICE site. We cannot rule out that a reduction in sea ice

cover (as inferred for substages 5e and 5a) was a regionally restricted phenomenon forced by a polynya-type setting (similar to the modern NorthEast Water Polynya, northeast Greenland).

[33] The knowledge of last interglacial paleoceanographic conditions in the interior Arctic Ocean is very limited. A number of last interglacial records from the Arctic shelf regions indicate a period of warmer conditions than today and a reduced sea ice cover [*Hamilton and Brigham-Grette*, 1991; *Brigham-Grette and Hopkins*, 1995; *Funder et al.*, 1998; *Kelly et al.*, 1999; *CAPE Last Interglacial Project Members*, 2006]. Dinocyst and benthic foraminifera studies from the northern Barents Sea margin suggest that Atlantic Water advection to the Arctic Ocean was somewhat stronger during the last interglacial [*Matthiessen and Knies*, 2001; *Matthiessen et al.*, 2001; *Wollenburg et al.*, 2001] and, during MIS 5a, possibly comparable to present conditions. However, evidence of relative warm last interglacial conditions at the northern Barents Sea margin contradicts the data on bulk carbonate, planktic foraminifera, and coccolith abundance from Fram Strait, which suggest a less intense Atlantic Water inflow than in the Holocene [*Gard and Backman*, 1990; *Köhler and Spielhagen*, 1990; *Hebbeln and Wefer*, 1997; *Bauch*, 1999]. An explanation for this discrepancy could be that low biogenic carbonate contents may be explained by dissolution and/or dilution with terrigeneous sediments. Mollusc and benthic foraminiferal data from last interglacial coastal deposits of Svalbard indicate conditions slightly warmer than the present [*Mangerud et al.*, 1998; *Bergsten et al.*, 1998]. These works and that of *Bauch* [1999], however, also argue that the last interglacial in that region appear to have been colder than the Holocene climatic optimum.

[34] Most of the circum-Arctic paleoclimate data mentioned above support that, in last interglacial Arctic Ocean records, small subpolar foraminifera (if preserved) should be found in larger abundances higher to the north than the present-day pattern. The GreenICE foraminiferal record indeed show this, and we may ask if the apparent dominance of polar specimens in other interior Arctic Ocean MIS 5 records is due to methodology (neglect of fine fraction: 63–125 μm), preferential preservation of thicker-shelled polar specimens, or regional differences in paleoceanographic conditions. Recent progress in Arctic Ocean late Quaternary stratigraphy and the identification of MIS 5e sediments in a number of key cores now call for an effort to solve this issue.

5.4. Glacial Ice Rafting

[35] The IRD records of cores 11 and 10 reveal specific periods of intensified deposition of IRD material possibly related to glacier collapse events during the last glacial-interglacial cycles. At the GreenICE site increased IRD deposition appear to have taken place during MIS 6 (early part and 6/5 transition, early-mid MIS 5 (5d?), MIS 4, and late MIS 3. For MIS 2 (including the Last Glacial Maximum) there is no evidence of intensified ice-rafting. This is in accordance with other interior Arctic Ocean MIS 2 records indicating extremely low sedimentation rates of clayey muds more or less barren in microfossils [*Darby et al.*, 1997; *Nørgaard-Pedersen et al.*, 1998, 2003]. The IRD material in cores 10 and 11 contains abundant detrital carbonates. This support a dominant terrestrial source from North Canada/Greenland where Palaeozoic platform carbonates extensively crops out [*Okulitch*, 1991; *Phillips and Grantz*, 2001]. Apart from the basal part of core 10, the IRD units show no similarity to the characteristic relatively thick IRD-rich units enriched in quartz grains known from the central Lomonosov Ridge, Makarov Basin, and the Morris Jesup Rise. These units have recently been dated to glacial stages MIS 6 and 4-3 [*Jakobsson et al.*, 2001; *Spielhagen et al.*, 2004]. In this respect, the GreenICE IRD record is more similar to Amerasian Basin records from the Northwind Ridge [e.g., *Phillips and Grantz*, 1997, 2001] and the Mendeleev Ridge [*Polyak et al.*, 2004]. Seismic records show possible glacial erosion of the top of the shallow (<550 m) Lomonosov Ridge about 45 km from the core sites [*Kristoffersen and Mikkelsen*, 2006]. There is no positive indication in the GreenICE record, though, supporting that this took place during the last two glacial-interglacial cycles. However, the circumstance that the longer cores are from deeper water (>1000 m) and that the other cores are very short (or only surface samples) limits the burden of proof for the timing of such erosion events.

6. Conclusions

[36] The GreenICE sediment records, from a hitherto unexplored area of the Arctic Ocean, reveal new data on variable Arctic Ocean paleoceanographic conditions during the last two glacial-interglacial cycles. The records contain very well preserved calcareous foraminifera and nannofossils allowing the establishment of a reliable age model and fix points for correlation with other interior Arctic Ocean late Quaternary records. The planktic foraminifera assemblage >63 μm reveals high abundances of small subpolar *T. quinqueloba* in the early and late interval of marine isotope stage 5. The abundance peaks are assigned to substage 5e (last interglacial) and 5a (warm interstadial). At present, this subpolar species occurs abundantly in subsurface Atlantic Waters close to the sea ice margin north of Svalbard and in the Barents Sea Branch. However, only a small percentage of subpolar specimens reach the interior Arctic Ocean as evidenced by living assemblages in the water column and late Holocene surface sediment samples from interior Arctic sites with excellent carbonate preservation. Even with an enhanced Atlantic Water boundary current system during the last interglacial period, it is unlikely that abundant subpolar specimens were advected several thousands kilometers to the interior Arctic Ocean. We therefore conclude that sea ice conditions near the GreenIce site must have been reduced during the last interglacial. Whether this was related to a polynya-type setting or reflects a generally reduced sea ice cover of the interior Arctic Ocean is not known at the present stage. Most circum-Arctic climate proxy data support interglacial conditions warmer than the present, but the few well-dated interior Arctic Ocean records preclude detailed reconstructions of paleoceanographic conditions. Studies of high-resolution interior and marginal Arctic Ocean records

potentially would inform us on the positions of paleo-ice margins and how variable sea ice conditions have been during recent warm periods. With respect to glacial conditions, increased ice-rafted debris deposition in the area appears to be associated with glacial stages 6, 4, and late 3, whereas stage 2 sediments (including Last Glacial Maximum) are condensed with a sparse IRD content only.

[37] **Acknowledgments.** We would like to thank all those who contributed with logistical assistance during the ice camp field campaign in May 2004. Special thanks go to John Boserup (GEUS) for his technical assistance and hard work under very difficult conditions. We extend our thanks to Robert Spielhagen (IFM-GEOMAR, Kiel) for allowing us to study radiocarbon-dated core top material from interior Arctic Ocean sites. This article was improved by the constructive comments of two anonymous reviewers. This contribution is a result of the EU GreenICE Project (EUK-2001-00280).

References

Aagard, K., J. H. Swift, and E. C. Carmack (1985), Thermohaline circulation in the arctic mediterranean seas, *J. Geophys. Res.*, *90*, 4833–4846.

Backman, J., M. Jakobsson, R. Løvlie, L. Polyak, and L. A. Febo (2004), Is the Central Arctic Ocean a sediment starved basin?, *Quat. Sci. Rev.*, *23*(11–13), 1435–1454.

Bauch, H. A. (1994), Significance of variability in *Turborotalita quinqueloba* (Natland) test size and abundance for paleoceanographic interpretations in the Norwegian-Greenland Sea, *Mar. Geol.*, *121*, 129–141.

Bauch, H. A. (1999), Planktic foraminifera in Holocene sediments from the Laptev Sea and the Central Arctic Ocean: Species distribution and paleobiogeographical implication, in *Land-Ocean Systems in the Siberian Arctic: Dynamics and History*, edited by H. Kassens et al., pp. 601–614, Springer, New York.

Bauch, H. A., H. Erlenkeuser, R. F. Spielhagen, U. Struck, J. Matthiessen, J. Thiede, and J. Heinemeier (2001), A multiproxy reconstruction of the evolution of deep and surface waters in the subarctic Nordic seas over the last 30000 years, *Quat. Sci. Rev.*, *20*(4), 659–678.

Bergsten, H., T. Anderson, and Ó. Ingólfsson (1998), Foraminiferal stratigraphy of raised marine deposits, representing isotope stage 5, Prins Karls Forland, western Svalbard, *Polar Res.*, *17*, 81–91.

Brigham-Grette, J., and D. M. Hopkins (1995), Emergent marine record and paleoclimate of the last interglaciation along the northwest Alaskan Coast, *Quat. Res.*, *43*, 159–173.

CAPE Last Interglacial Project Members (2006), Last Interglacial arctic warmth confirms polar amplification of climate change, *Quat. Sci. Rev.*, *25*(13–14), 1552–1569.

Carstens, J., and G. Wefer (1992), Recent planktonic foraminifera in the Nansen Basin, Arctic Ocean, *Deep Sea Res., Part A*, *39*(2), 507–524.

Carstens, J., D. Hebbeln, and G. Wefer (1997), Distribution of planktic foraminifera at the ice margin in the Arctic (Fram Strait), *Mar. Micropaleontol.*, *29*, 257–269.

Clark, D. L., R. R. Whitman, K. A. Morgan, and S. D. Mackey (1980), Stratigraphy and glacial-marine sediments of the Amerasian Basin, central Arctic Ocean, *Spec. Pap. Geol. Soc. Am.*, *181*, 57 pp.

Darby, D. A., J. F. Bischof, and G. A. Jones (1997), Radiocarbon chronology of depositional regimes in the western Arctic Ocean, *Deep Sea Res., Part II*, *44*(8), 1745–1757.

de Vernal, A., and C. Hillaire-Marcel (2005), Variability of sea ice cover in the Chukchi Sea (western Arctic Ocean) during the Holocene, *Paleoceanography*, *20*, PA4018, doi:10.1029/2005PA001157.

Dokken, T. M., and M. Hald (1996), Rapid climatic shifts during isotope stages 2–4 in the polar north Atlantic, *Geology*, *24*, 599–602.

Environmental Working Group (1997), *Environmetal Working Group Joint U.S.-Russian Atlas of the Arctic Ocean* [CD-ROM], Natl. Snow and Ice Data Cent., Boulder, Colo.

Foley, K. M., and R. Poore (1993), Planktic foraminifer census data from Northwind Ridge core 5 Arctic Ocean, *U.S. Geol. Surv. Open File Rep.* 91-346.

Funder, S., C. Hjort, J. Y. Landvik, S.-I. Nam, N. Reeh, and R. Stein (1998), History of a stable ice margin: East Greenland during the Middle and Upper Pleistocene, *Quat. Sci. Rev.*, *17*, 77–123.

Gard, G. (1988), Late Quaternary calcareous nannofossil biozonation, chronology and palaeo-oceanography in areas north of the Faeroe-Iceland Ridge, *Quat. Sci. Rev.*, *7*, 65–78.

Gard, G., and J. Backman (1990), Synthesis of Arctic and Sub-Arctic coccolith biochronology and history of North Atlantic Drift water influx during the last 500000 years, in *Geological History of the Polar Oceans: Arctic Versus Antarctic, NATO ASI Ser.*, *Ser. C*, vol. 308, edited by U. Bleil and J. Thiede, pp. 417–436, Springer, New York.

Haas, C., S. Hendricks, and M. Doble (2006), Comparison of the sea ice thickness distribution in the Lincoln Sea and adjacent Arctic ocean in 2004 and 2005, *Ann. Glaicol*, *44*, in press.

Haflidason, H., J. Eiriksson, and S. Van Kreveld (2000), The tephrachronology of Iceland and the North Atlantic region during the middle and late Quaternary: A review, *J. Quat. Sci.*, *15*, 3–22.

Hald, M., H. Ebbesen, M. Forwick, F. Godtliebsen, L. Khomenko, S. Korsun, L. Ringstad Olsen, and T. O. Vorren (2004), Holocene paleoceanography and glacial history of the West Spitsbergen area, Euro-Arctic margin, *Quat. Sci. Rev.*, *23*, 2075–2088.

Hamilton, T. D., and J. Brigham-Grette (1991), The last interglaciations in Alaska: Stratigraphy and paleoecology of potential sites, *Quat. Int.*, *10–12*, 49–71.

Hebbeln, D., and G. Wefer (1997), Late Quaternary paleoceanography in the Fram Strait, *Paleoceanography*, *12*(1), 65–78.

Hebbeln, D., T. Dokken, E. S. Andersen, M. Hald, and A. Elverhøi (1994), Moisture supply for northern ice-sheet growth during the Last Glacial Maximum, *Nature*, *370*, 357–360.

Hommers, H. (1998), Gehäuseuntersuchungen an planktischen Foraminiferen hoher Breiten, Hinweise auf Umweltveränderungen während der letzten 140.000 Jahre, *Rep. Polar Res. 295*, 96 pp., Alfred Wegener Inst. for Polar and Mar. Res., Bremerhaven, Germany.

Ishman, S. E., L. Polyak, and R. Z. Poore (1996), An expanded record of Pleistocene deep Arctic change: Canada Basin, western Arctic Ocean, *Geology*, *24*, 139–142.

Jakobsson, M., R. Løvlie, H. Al-Hanbali, E. Arnold, J. Backman, and M. Mörth (2000), Manganese and color cycles in Arctic Ocean sediments constrain Pleistocene chronology, *Geology*, *28*, 23–26.

Jakobsson, M., R. Løvlie, E. Arnold, J. Backman, L. Polyak, L. Knutsen, and E. Musatov (2001), Pleistocene stratigraphy and paleoenvironmental variation from Lomonosov Ridge sediments, central Arctic Ocean, *Global Planet. Change*, *31*, 1–21.

Jakobsson, M., J. Backman, A. Murray, and R. Løvlie (2003), Optically stimulated luminescence dating supports central Arctic Ocean cm-scale sedimentation rates, *Geochem. Geophys. Geosyst.*, *4*(2), 1016, doi:10.1029/2002GC000423.

Johannessen, T., E. Jansen, A. Flatoy, and A. C. Ravelo (1994), The relationship between surface water masses, oceanographic fronts, and paleoclimatic proxies in surface sediments of the Greenland, Iceland Norwegian seas, in Carbon Cycling in the Glacial Ocean: Constraints on the Ocean's Role in Global Change, edited by R. Zahn et al., *NATO ASI Ser.*, *Ser. I*, vol. 117, pp. 61–85, Springer, New York.

Johannessen, O. M., et al. (2004), Arctic climate change: Observed and modeled temperature and sea-ice variability, *Tellus, Ser. A*, *56*(5), 559–560.

Kandiano, E. S., and H. A. Bauch (2002), A case study on the application of different planktic foraminiferal size fractions for interpreting late Quaternary paleoceanographic changes in the polar North Atlantic, *J. Foraminiferal Res.*, *32*(3), 245–251.

Kelly, M., S. Funder, M. Houmark-Nielsen, K. L. Knudsen, C. Kronborg, J. Landvik, and L. Sorby (1999), Quaternary glacial and marine environmental history of northwest Greenland: A review and reappraisal, *Quat. Sci. Rev.*, *18*, 373–392.

Knies, J., N. Nowaczyk, C. Müller, C. Vogt, and R. Stein (2000), A multiproxy approach to reconstruct the environmental changes along the Eurasian continental margin over the last 150.000 years, *Mar. Geol.*, *163*, 317–344.

Köhler, S. E. I., and R. F. Spielhagen (1990), The enigma of oxygen isotope stage 5 in the central Fram Strait, in *Geological History of the Polar Oceans: Arctic Versus Antarctic, NATO ASI Ser., Ser. C*, vol. 308, edited by U. Bleil and J. Thiede, pp. 489–497, Springer, New York.

Kristoffersen, Y., and N. Mikkelsen (2006), On sediment deposition and nature of the plate boundary at the junction between the submarine Lomonosov Ridge, Arctic Ocean and the continental margin of Arctic Canada/North Greenland, *Mar. Geol.*, *225*, 265–278.

Lea, D. A., P. A. Martin, D. K. Pak, and H. Spero (2002), Reconstructing a 350 ky history of sea level using planktonic Mg/Ca and oxygen iso-

tope records from a Cocos Ridge core, *Quat. Sci. Rev.*, *21*, 283–293.

Mangerud, J., and S. Gulliksen (1975), Apparent radiocarbon ages of recent marine shells from Norway, Spitsbergen, and Arctic Canada, *Quat. Res.*, *5*, 263–273.

Mangerud, J., T. Dokken, D. Hebbeln, B. Heggen, Ó. Ingólfsson, J. Y. Landvik, V. Mejdahl, J.-I. Svendsen, and T. Vorren (1998), Fluctuations of the Svalbard-Barents Sea ice sheet during the last 150000 years, *Quat. Sci. Rev.*, *17*, 11–42.

Matthiessen, J., and J. Knies (2001), Dinoflagellate cyst evidence for warm interglacial conditions at the northern Barents Sea margin during marine isotope stage 5, *J. Quat. Sci.*, *16*(7), 727–737.

Matthiessen, J., J. Knies, N. R. Nowaczyk, and R. Stein (2001), Late Quaternary dinoflagellate cyst stratigraphy at the Eurasian continental margin, Arctic Ocean: Indications for Atlantic water inflow in the past 150000 years, *Global Planet. Change*, *31*(1–4), 65–86.

Minicucci, D. A., and D. L. Clark (1983), A Late Cenozoic stratigraphy for glacial-marine sediments of the eastern Alpha Cordillera, central Arctic Ocean, in *Glacial-Marine Sedimentation*, edited by B. F. Molnia, pp. 331–365, Springer, New York.

Nørgaard-Pedersen, N., R. F. Spielhagen, J. Thiede, and H. Kassens (1998), Central Arctic surface ocean environment during the past 80000 years, *Paleoceanography*, *13*(2), 193–204.

Nørgaard-Pedersen, N., R. F. Spielhagen, H. Erlenkeuser, P. M. Grootes, J. Heinemeier, and J. Knies (2003), The Arctic Ocean during the Last Glacial Maximum: Atlantic and Polar domains of surface water mass distribution and ice cover, *Paleoceanography*, *18*(3), 1063, doi:10.1029/2002PA000781.

ACIA Overview Report (2004), *Impacts of a Warming Arctic: Arctic Climate Impact Assessment*, 144 pp., Cambridge Univ. Press, New York.

Okulitch, A. V. (Comp.) (1991), Geology of the Canadian archipelago and north Greenland, in *The Geology of North America*, vol. E., *Geology of the Innuitian Orogen and Arctic Platform of Canada and Greenland*, edited by H. P. Trettin, Figure 2, scale 1:200.000, Geol. Soc. Am., Boulder, Colo.

Phillips, R. L., and A. Grantz (1997), Quaternary history of sea ice and paleoclimate in the Amerasia basin, Arctic Ocean, as recorded in the cyclical strata of Northwind Ridge, *Geol. Soc. Am. Bull.*, *109*, 1101–1115.

Phillips, R. L., and A. Grantz (2001), Regional variations in provenance and abundance of ice-rafted clasts in Arctic Ocean sediments: Implications for the configuration of Late Quaternary oceanic and atmospheric circulation in the Arctic, *Mar. Geol.*, *172*, 91–115.

Polyak, L., W. B. Curry, D. A. Darby, J. Bischof, and T. M. Cronin (2004), Contrasting glacial/interglacial regimes in the western Arctic Ocean as exemplified by a sedimentary record from the Mendeleev Ridge, *Palaeogeogr. Palaeoclimatol. Palaeoecol.*, *20*, 73–93.

Poore, R. Z., R. L. Phillips, and H. J. Rieck (1993), Paleoclimate record for Northwind Ridge, western Arctic Ocean, *Paleoceanography*, *8*(2), 149–159.

Poore, R. Z., L. Osterman, W. B. Curry, and R. L. Phillips (1999), Late Pleistocene and Holocene meltwater events in the western Arctic Ocean, *Geology*, *27*, 759–762.

Rothrock, D. A., Y. Yu, and G. A. Maykut (1999), Thinning of the Arctic sea-ice cover, *Geophys. Res. Lett.*, *26*(23), 3469–3472.

Rudels, B., A.-M. Larsson, and P.-I. Sehlstedt (1991), Stratification and water mass formation in the Arctic Ocean: Some implications for the nutrient distribution, *Polar Res.*, *10*, 19–32.

Rudels, B., E. P. Jones, L. G. Anderson, and G. Kattner, (1994). On the intermediate depth waters of the Arctic Ocean, in *The Polar Oceans and Their Role in Shaping the Global Environment, Geophys. Monogr. Ser.*, vol. 85, edited by O. M. Johannesen, R. D. Muench and J. E. Overland, pp. 33–46, AGU, Washington, D. C.

Rudels, B., H. J. Friederich, and D. Quadfasel (1999), The Arctic Circumpolar Boundary Current, *Deep Sea Res., Part II*, *46*, 1023–1062.

Scott, D. B., P. J. Mudie, V. Baki, K. D. MacKinnon, and F. E. Cole (1989), Biostratigraphy and Late Cenozoic paleoceanography of the Arctic Ocean: Foraminiferal, lithostratigraphic, and isotopic evidence, *Geol. Soc. Am. Bull.*, *101*, 260–277.

Spielhagen, R. F., and H. Erlenkeuser (1994), Stable oxygen and carbon isotopes in planktic foraminifers from Arctic Ocean surface sediments: Reflection of the low salinity surface water layer, *Mar. Geol.*, *119*(3/4), 227–250.

Spielhagen, R. F., et al. (1997), Arctic Ocean evidence for Late Quaternary initiation of northern Eurasian ice sheets, *Geology*, *25*, 783–786.

Spielhagen, R. F., K.-H. Baumann, H. Erlenkeuser, N. R. Nowaczyk, N. Nørgaard-Pedersen, C. Vogt, and D. Weiel (2004), Arctic Ocean deep-sea record of northern Eurasian ice sheet history, *Quat. Sci. Rev.*, *23*, 1455–1483.

Stein, R., C. Vogt, C. Schubert, and D. Fütterer (1994), Stable isotope stratigraphy, sedimentation rates, and salinity changes in the latest Pleistocene to Holocene eastern central Arctic Ocean, *Mar. Geol.*, *119*, 333–355.

Steinsund, P. I., and M. Hald (1994), Recent calcium carbonate dissolution in the Barents Sea: Paleoceanographic implications, *Mar. Geol.*, *117*, 303–316.

Thierstein, H. R., K. Geitzenauer, B. Molfino, and N. J. Shackleton (1977), Global synchroneity of late Quarternary coccolith datum levels: Validation by oxygen isotopes, *Geology*, *5*, 400–404.

Voelker, A. H. L., M. Sarnthein, P. M. Grootes, H. Erlenkeuser, C. Laj, A. Mazaud, M.-J. Nadeau, and M. Schleicher (1998), Correlation of marine ^{14}C ages from the Nordic Seas with the GISP2 isotope record: Implications for ^{14}C calibration beyond 25 ka BP, *Radiocarbon*, *40*(1), 517–534.

Volkmann, R. (2000a), Planktic foraminifers in the outer Laptev Sea and the Fram Strait: Modern distribution and ecology, *J. Foraminiferal Res.*, *30*, 157–176.

Volkmann, R. (2000b), Planktic foraminifer ecology and stable isotope geochemistry in the Arctic Ocean: Implications from water column and sediment surface studies for quantitative reconstructions of oceanic parameters, *Rep. Polar Res. 361*, 100 pp., Alfred Wegener Inst. for Polar and Mar. Res., Bremerhaven, Germany.

Wadhams, P. (1997), Ice thickness in the Arctic Ocean: The statistical reliability of experimental data, *J. Geophys. Res.*, *102*, 27,951–27,959.

Wadhams, P., and N. R. Davis (2000), Further evidence of ice thinning in the Arctic Ocean, *Geophys. Res. Lett.*, *27*, 3973–3975.

Wollenburg, J., W. Kuhnt, and A. Mackensen (2001), Changes in Arctic Ocean paleoproductivity and hydrography during the last 145 kyr: The benthic foraminiferal record, *Paleoceanography*, *16*(1), 65–77.

Y. Kristoffersen, Department of Earth Science, University of Bergen, N-5007 Bergen, Norway.

S. J. Lassen, N. Mikkelsen, N. Nørgaard-Pedersen, and E. Sheldon, Geological Survey of Denmark and Greenland, Øster Voldgade 10, DK-1350 Copenhagen, Denmark. (nnp@geus.dk)